# Synthesis and Characterization of Polymer-Coated Quantum Dots with Integrated Acceptor Dyes as FRET-Based Nanoprobes

**11 AUTHORS**, INCLUDING:

Jean-Maurice Mallet

Pierre and Marie Curie University - Paris 6

**178** PUBLICATIONS **2,597** CITATIONS

SEE PROFILE

Anne Feltz

Ecole Normale Supérieure de Paris

**104** PUBLICATIONS **3,178** CITATIONS

SEE PROFILE

Martin Oheim

French National Centre for Scientific Research

**63** PUBLICATIONS **2,155** CITATIONS

SEE PROFILE

Wolfgang J. Parak

Philipps University of Marburg

**360** PUBLICATIONS **18,130** CITATIONS

SEE PROFILE

# Synthesis and Characterization of Polymer-Coated Quantum Dots with Integrated Acceptor Dyes as FRET-Based Nanoprobes

**María Teresa Fernández-Argüelles,[†,‡,§] Aleksey Yakovlev,[†,ǁ] Ralph A. Sperling,[‡]
Camilla Luccardini,[⊥] Stéphane Gaillard,[+] Alfredo Sanz Medel,[§]
Jean-Maurice Mallet,[+] Jean-Claude Brochon,[#] Anne Feltz,*[,ǁ] Martin Oheim,*[,⊥] and
Wolfgang J. Parak*[,‡]**

*Center for Nanoscience, Ludwig-Maximilans Universität Munich, Amalienstrasse 54,
Munich, D-80799 München, Germany, Fakultät Physik, Philipps Universität Marburg,
Renthof 7, 35037 Marburg, Germany, Analytical Spectrometry Research Group,
Department of Physical and Analytical Chemistry, University of Oviedo,
c/Julián Clavería, 8. Oviedo, ES-33006 Spain, ENS-CNRS UMR 8544,
Laboratoire de Neurobiologie, Département de Biologie, Ecole Normale Supérieure,
46 rue d'Ulm, Paris, F-75005 France, INSERM S603, Paris, F-75006 France,
University Paris Descartes, Laboratory of Neurophysiology and New Microscopies,
45 rue des Saints Pères, Paris, F-75006 France, ENS-CNRS UMR 8642, Glycoscience,
Département de Chimie, 24 rue Lhomond, Paris, F-75231 France, and Laboratoire de
Biotechnologies et Pharmacologie génétique Appliquée (LBPA) ENS-CNRS UMR 8113,
Ecole Normale Supérieure de Cachan, 61 avenue du President Wilson,
Cachan, F-94235 France*

## ABSTRACT

A fluorescence resonance energy transfer pair consisting of a colloidal quantum dot donor and multiple organic fluorophores as acceptors is reported and the photophysics of the system is characterized. Most nanoparticle-based biosensors reported so far use the detection of specific changes of the donor/acceptor distance under the influence of analyte binding. Our nanoparticle design on the other hand leads to sensors that detect spectral changes of the acceptor (under the influence of analyte binding) at fixed donor/acceptor distance by the introduction of the acceptor into the polymer coating. This approach allows for short acceptor–donor separation and thus for high-energy transfer efficiencies. Advantageously, the binding properties of the hydrophilic polymer coating further allows for addition of poly(ethylene glycol) shells for improved colloidal stability.

Fluorescence resonant energy transfer (FRET)-based semiconductor nanocrystal (NC) sensors have emerged over the past years as promising nanoscale sensors for analyte detection.[1–5] Apart from their larger absorption cross sections and higher photostability when compared with organic fluorophores, the interest in NCs as FRET donors particularly stems from the reduced spectral cross-talk between donor and acceptor signals. The possibility of an efficient blue-shifted donor excitation at wavelengths remote from acceptor, direct excitation minimizes cross-excitation, and the size-tunable donor emission allows for optimal spectral overlap with acceptor absorption. At the same time, the narrow symmetric donor spectrum alleviates the common problem of donor red tailing into acceptor emission wavelengths. With only few exceptions,[6] the NC typically has been used as a central donor and scaffold for the attachment of multiple

---

* Corresponding authors: Anne Feltz, anne.feltz@ens.fr; Martin Oheim, martin.oheim@univ-paris5.fr; Wolfgang Parak, wolfgang.parak@physik.uni-marburg.de.
† These authors contributed equally.
‡ Center for Nanoscience, Ludwig-Maximilans Universität Munich and Fakultät Physik, Philipps Universität Marburg.
§ Analytical Spectrometry Research Group, Department of Physical and Analytical Chemistry, University of Oviedo.
ǁ ENS-CNRS UMR 8544, Laboratoire de Neurobiologie, Département de Biologie, Ecole Normale Supérieure.
⊥ INSERM S603 and University Paris Descartes.
+ ENS-CNRS UMR 8642, Glycoscience, Département de Chimie.
# Laboratoire de Biotechnologies et Pharmacologie génétique Appliquée (LBPA), ENS-CNRS UMR 8113, Ecole Normale Supérieure de Cachan.

organic fluorophores or quenchers. In many of these nanosensors, the acceptors are coupled via receptor−ligand interaction, by linking the receptor to the NC and the ligand to the organic acceptor/quencher. The presence of an analyte engenders a change of the donor/acceptor distance that is measured as a change in the FRET efficiency, either in intensity measurements as donor quenching or sensitized acceptor fluorescence or as a decrease in the donor lifetime. Several strategies for analyte-mediated distance changes have been demonstrated: (1) The analyte acts as a competitive ligand for receptor binding by displacing the original fluorescent ligand.[7,8] (2) The analyte specifically cleaves the linkage between the NC donor and the acceptor.[9,10] (3) The analyte mediates the binding of the acceptor to the donor.[11,12] (4) The analyte changes the conformation of the linkage between the donor and the acceptor.[13] These sensor geometries have in common that the FRET contrast is based on (reversibly or irreversibly) displacing the acceptor from the NC donor.

In an alternative sensor configuration, the acceptor is statically bound on the NC surface and analyte binding/unbinding rather changes the overlap integral between donor emission and acceptor excitation and thus modifies the FRET efficiency.[14] Thus, rather than changing the donor/acceptor distance, the acceptor fluorophore conveys its indicator function to the FRET pair. Finally, one can imagine a slightly modified configuration in which the donor constantly transfers energy to the acceptor, the fluorescence emission of which is changed through a modulation of its quantum efficiency upon ligand binding.

For such static systems to provide sufficient signal and stability, the acceptor should be linked as close to the donor as possible, and the linkage should be stable. Furthermore, sufficient colloidal stability is desirable, which goes hand in hand with stable linkage. Unfortunately there is a tradeoff between both demands. When the acceptor is directly linked to the surfactant-stabilized NC surface through partial ligand exchange, then the acceptor will be as close as possible to the particle surface. Yet, surfactant-stabilized NCs have only limited long-term stability in aqueous solution and tend to aggregate, as eventually the ligands and hence also the acceptor will unbind from the donor.[15] Alternatively, embedding the NC donor in a more complex shell, such as encapsulation between zipper proteins,[16] in a cross-linked ligand shell,[17] in a glass shell,[18] in micelles,[19] or in a polymer coat,[20−24] and the subsequent functionalization with poly-(ethylene glycol) (PEG)[25,26] permit a good colloidal stability but increases the effective diameter of the nanoparticle[24,27−30] and hence donor/acceptor separation distance. While the polymer shell adds on the order of 3−4 nm to the particle radius,[30] additional coating with PEG adds another few nanometers.[30] The resulting donor/acceptor distances are hence much larger than typical Förster radii, which are on the order of a nanometer so that colloidally stable (PEG-coated) NC-based biosensors typically have lower FRET efficiencies and signal.

In this study, we introduce a FRET geometry in which the acceptor is directly incorporated into the encapsulation
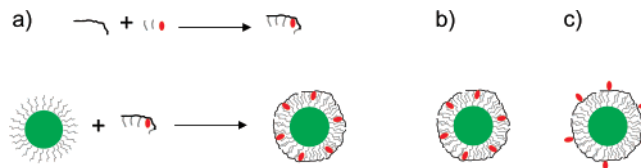


**Figure 1.** (a) An amphiphilic polymer is synthesized by reacting hydrophobic hydrocarbon chains (dark gray) and an organic dye (red) to a polar polymer backbone (light gray). Quantum dots (inorganic CdSe/ZnS core/shell drawn in green capped with trioctylphosphine oxide and similar surfactants drawn in dark gray) are coated with the amphiphilic polymer by intercalation of the hydrophobic side chains of the polymer with the hydrophobic surfactant molecules on the quantum dot surface and the resultant polymer-coated quantum dot is hydrophilic due to the polar polymer backbone.[21] The following dye/quantum dot configurations were used in this study: (b) polymer-coated quantum dots with dye incorporated in the polymer; (c) polymer-coated quantum dots with dye linked to the polymer shell with a postmodification process.

shell used to provide colloidal stability to the NC donor. In this way, the linkage of the acceptor to the NC donor is very stable, the whole assembly has excellent colloidal stability, and the donor/acceptor distance is potentially reduced. We here compare the performance of this system to assemblies reported so far, in which the acceptor has been linked in a postmodification to the outside of a polymer shell around the NC donor.

An amphiphilic polymer is synthesized by linking amino-functionalized hydrophobic hydrocarbon chains (dodecy-lamine) to a polar backbone (poly(isobutylene-*alt*-maleic anhydride), $M_w = 6$ kDa) under reaction of the amino group of the hydrocarbon chain with the anhydride rings of the polymer backbone (reaction in anhydrous tetrahydrofuran; the quantity of dodecylamine is calculated in a way that 75% of the anhydride rings react with one dodecylamine molecule each; for a detailed protocol see Supporting Information).[20,31,32] The acceptor fluorophore (amino-modified ATTO590) was incorporated into the amphiphilic polymer by reaction of the amino group of the dye with the anhydride rings of the polymer backbone (reaction in anhydrous chloroform; the quantity of dye is calculated in a way that 1% (or alternatively 2%, 4%, or 8%) of the anhydride rings react with one dye molecule each, see Figure 1a. CdSe/ZnS quantum dots (Qdot 545 ITK organic quantum dots, Invitrogen, # Q21791MP) were then coated with the dye (ATTO590)-modified amphiphilic polymer according to a previously published protocol (see Figure 1a,b).[21] The particles are colloidally stabilized in aqueous solution by negatively charged carboxyl groups originating from opened anhydride rings. Assuming a Förster-type $r^{-6}$ interaction between Qdot 545 ITK and ATTO590, we estimate from their overlap integral a Förster radius of 6.4 nm. As a control, we coated under the same conditions Qdots 545 ITK with amphiphilic polymer devoid of ATTO dye. In one set of experiments, we linked to these particles ATTO dye in a postmodification procedure with EDC chemistry (linkage of the amino group of the amino-modified ATTO590 with the carboxyl groups of the polymer, mediated by *N*-(3-dimethyl-aminopropyl)-*N*′-ethylcarbodiimide hydrochloride, see Figure 1c). We note that the polymer-coating procedure

**Figure 2.** Quantum dots were coated with an amphiphilic polymer without (2) and with (3) incorporated ATTO590 dye. As control, empty polymer micelles with incorporated dye (1) are used. The three samples were loaded on a 1% agarose gel (arrow), and a voltage of 100 V was applied for around 1 h. During this time the negatively charged particles migrated toward the plus pole. Fast (F) and slow (S) migrating bands were observed by illumination the gel with a hand-held UV lamp. The empty polymer micelles (lane 1) can be seen as "fast" band by the red fluorescence of the ATTO dye incorporated in the polymer. The polymer coated quantum dots (without dye in the polymer, lane 2) can be seen as "slow" band by the green fluorescence of the quantum dots. Presumably, the polymer-coating procedure also produces empty micelles, which are not fluorescent and are not detected in our assay. The sample with the polymer coated quantum dots with dye incorporated in the polymer (lane 3) yields one "slow" band with orange fluorescent and one "fast" band with red fluorescence. The fast band (which migrated at the same speed as the control sample (1) with the empty polymer micelles) can be attributed to empty polymer micelles, which had been formed during the polymer coating process, and they can be observed due to the fluorescence of the ATTO dye incorporated in the polymer. The slow band (which migrated at the same speed as the polymer-coated quantum dots (2)) can be attributed to polymer coated quantum dots with dye incorporated in the polymer. The emission from these nanoparticles appears orange, as part of the energy absorbed by the quantum dots is transferred via FRET to the dye in the polymer, and for this reason an overlap of the quantum dot and dye fluorescence is observed.

results in some empty polymer micelles[32] in addition to polymer-coated particles. In contrast to earlier reports for a similar system[33] size-exclusion chromatograpy failed to separate excess polymer (in the form of micelles) from the polymer-coated NCs. However, gel electrophoresis[18] reliably separated the polymer micelles (see Figure 2). We used for all spectroscopic measurements NCs that were purified from excess micelles by gel electrophoresis.

To characterize the efficiency of energy transfer from the NC donor to the ATTO590 acceptor, we measured both spectrally resolved intensities (Figure 3a) and fluorescence decays, using a time-correlated single photon counting (TCSPC) approach[34] (Figure 3b). Lifetime measurements allow the FRET measurement independent of the donor concentration, by calculating $E = 1 - \langle\tau_{DA}\rangle/\langle\tau_D\rangle$, where $\tau_{DA}$ and $\tau_D$ are the donor lifetimes in the presence and absence of the acceptor, respectively, and $\langle \rangle$ denotes the weighted average over all lifetime components, see Figure 3b and Supporting Information for details.

The measured absorption spectra of the QD545/ATTO590 conjugates were dominated by the acceptor absorption. In the 550−600 nm range, the contribution of the NC to the total absorption was barely detected so that we could not determine the donor/acceptor ratio from absorbance measure-

ments (see Supporting Information for details). With NCs and ATTO molecules having an absorbance of 156 000 vs 22 000 M$^{-1}$ cm$^{-1}$ at 450 nm, respectively, and ∼15% noise, we can estimate that at least 47 ATTO590 molecules are required to obscure the NC absorption. This number is plausible in view of the number of dye molecules that have been added during the polymer coating (≤56 ATTO molecules per quantum dot in the case that only 1% of these anhydride sites were occupied with dye). Thus, for the case of the polymer with the least attached ATTO molecules (1% of the sites), each NC donor is decorated with about 50 ATTO dye acceptors.

In as much as we could determine the ATTO590 dye concentration but not the exact stoichiometry (donor/acceptor ratio) for the QD545/ATTO590 conjugates, we first normalized all measured fluorescence emission spectra to the (total) number of ATTO590 molecules, in the NC polymer coat or free in solution. To estimate the total number of ATTO590 molecules, we first directly excited the ATTO590 acceptor at 590 nm (where little interference from donor fluorescence is expected). Each of the emission spectra of the donor/acceptor conjugates, recorded at 450 nm excitation (where direct excitation of ATTO590 is low) was normalized by division through the peak fluorescence measured at 590 nm excitation (Figure 3). This first normalization scales the curves to an equal quantity of acceptors. Next, to account for fluctuations in the excitation power we further scaled the normalized emission spectra of the ATTO dye in the absence of the QD545, excited at 450 nm to a peak emission of 1.

Figure 3a displays these doubly normalized fluorescence emission spectra for the different QD545/ATTO590 dye assemblies, measured in 1 cm cuvettes. The red curve corresponds to empty micelles devoid of NCs but with ATTO dye embedded in the polymer. The spectral emission of the ATTO dye did not change by embedding it into the amphiphilic polymer, as the micelle spectrum matches that of the normalized spectrum of free ATTO590 dye (data shown in Supporting Information). The orange trace represents QD545 nanoparticles with ATTO590 dye incorporated in the polymer shell. Two emission peaks are readily apparent. The emission peak in the green/yellow (545 nm) corresponds to the NC donor, the one in the red (622 nm) to the ATTO590 acceptor. Part of the energy absorbed by the NCs is directly emitted (fluorescence emission of the quantum dots in the green/yellow) and another part is transferred by FRET to the ATTO dye, from where it also can be emitted (fluorescence emission of the ATTO dye in the red). The emission intensity of the ATTO dye bound to the NC is more than five times larger than the direct excitation of free ATTO dye molecules, indicating sensitized acceptor fluorescence due to FRET. Time-resolved measurements corroborated this interpretation. Using femtosecond-pulsed-laser exciation at 450 nm, we measured the fluorescence decay of the emission of the NCs, Figure 3b. Weighted average decay times of bare polymer coated NCs without the ATTO dye (green curve) were around 10 ns. FRET offered an alternative pathway for donor relaxation, reducing
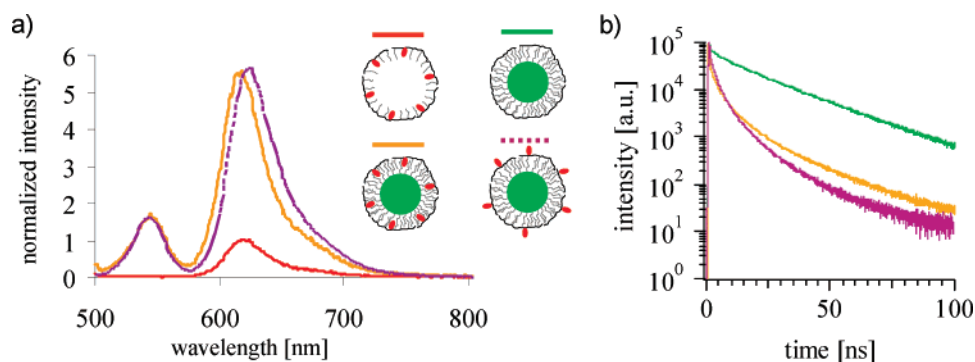
**Figure 3.** Spectroscopic characterization of different samples. (a) Normalized fluorescence intensity upon excitation at 450 nm. The spectra were normalized in a way that they all refer to solutions with the same amount of ATTO dye molecules and that the emission intensity of free ATTO dye is 1. (b) Normalized fluorescence decays. The pulse rate of a frequency-doubled Ti:sapphire laser was reduced to 4 MHz to accommodate the long NC decay times. Traces are normalized to $10^5$ counts at peak. The noise under these conditions was on the order of $10^0$.

its lifetime to about 2 ns in the presence of ATTO dye embedded in the polymer shell (orange trace).

In addition to NCs containing ~50 ATTO molecules per donor (1%), we also prepared conjugates with an amphiphilic polymer layer in which 4% and 8% of the anhydride rings had been reacted with amino-modified ATTO dye. Increasing the amount of dye embedded in the polymer during synthesis decreased the measured average donor lifetime from 2.5 ns (1%) to 2.1 (4%) and 1.7 ns (8%). The corresponding FRET efficiencies are estimated as 0.75, 0.79, and 0.84, respectively. This observation is in line with the measured normalized emission spectra for these conjugates (orange line on Figure 3a). With the peak emission of the acceptor normalized as above, the peak at donor emission is getting increasingly smaller when increasing the ATTO concentration from 1% to 8%.

When the ATTO dye is linked via EDC chemistry to the polymer shell of the NCs (see Figure 1b for a schematic representation), the normalized intensity as well as the photoluminescence decay time (dotted purple traces in parts a and b of Figure 3, respectively) were comparable to those obtained with ATTO dye within the polymer shell (straight orange line). However, the fluorescence emission peak was ~10 nm red-shifted compared to the pure ATTO590 dye or the other tested geometries, probably due to a change in the local microenvironment of the dye. As before, we equally varied the donor/acceptor ratio by increasing their concentration ratio during synthesis. Again, the FRET efficiencies systematically increased when increasing the acceptor concentration. There is no significant difference in FRET efficiency and hence donor/acceptor distance between including the ATTO during synthesis or adding it afterward to the polymer shell. FRET efficiencies ranged between 0.77 and 0.84 and were thus not markedly different from the conjugates in which the acceptor was directly included into the polymer coat. Thus, the sketches in Figure 1 are probably too idealized. Nevertheless, there are several distinctive advantages of embedding the dye into the polymer shell rather than adding it afterward to the polymer shell. First, acceptor binding was very efficient, as basically all used ATTO molecules were incorporated into the polymer shell.

Second, in contrast to postmodification in aqueous solution, which requires a water-soluble dye, also hydrophobic dyes can be readily incorporated into the polymer shell, as the actual synthesis of the amphiphilic polymer is performed in organic solvent. Third, problems with colloidal stability are equally circumvented when adding the dye directly into the polymer shell, as no condition with high salt concentration as needed for EDC chemistry is required. Thus, from a practical standpoint, the inclusion of the acceptor facilitates shipping the conjugates to the end user and permits a long shelf life, without concerns about the sensor stability.

In conclusion, our experiments indicate that embedding the acceptor dye directly in the amphiphilic polymer used to make the donor nanoparticle water soluble leads to a novel and advantageous geometry that can be used for FRET-based nanosensors, for which the acceptor needs to be statically fixed to the donor.[14] This assembly is known to provide an excellent colloidal stability[21,26] and it allows for all postmodification steps that have been already demonstrated for polymer-coated particles. In particular, the polymer-coated NCs (with the dye incorporated into the polymer shell) could be further colloidally stabilized with an additional PEG shell and also be modified with a precisely controlled number of functional groups.[26] This makes them promising candidates for the investigation of cellular traffic on a single particle level.[35,36]

**Supporting Information Available:** Descriptions of synthesis of the amphiphilic polymer, polymer coating of quantum dots, sample purification with gel electrophoresis, normalization procedure for the evaluation of fluorescence

spectra, evaluation of the fluorescence spectra, and time resolved measurements. This material is available free of charge via the Internet at http://pubs.acs.org.

## References

(1) Medintz, I. L.; Uyeda, H. T.; Goldman, E. R.; Mattoussi, H. *Nat. Mater.* **2005**, *4* (6), 635−446.

(2) Clapp, A. R.; Medintz, I. L.; Mattoussi, H. *ChemPhysChem* **2006**, *7*, 47−57.

(3) Dubertret, B. *Nat. Mater.* **2005**, *4*, 797−798.

(4) Medintz, I. L.; Deschamps, J. R. *Curr. Opin. Biotechnol.* **2006**, *17* (1), 17−27.

(5) Lin, C.-A. J.; Liedl, T.; Sperling, R. A.; Fernández-Argüelles, M. T.; Costa-Fernández, J. M.; Pereiro, R.; Sanz-Medel, A.; Chang, W. H.; Parak, W. J. *J. Mater. Chem.* **2007**, *17* (14), 1343−1346.

(6) So, M.-K.; Xu, C.; Loening, A. M.; Gambhir, S. V.; Rao, J. *Nat. Biotechnol.* **2006**, *24* (3), 339−343.

(7) Medintz, I. L.; Clapp, A. R.; Mattoussi, H.; Goldman, E. R.; Fisher, B.; Mauro, J. M. *Nat. Mater.* **2003**, *2*, 630−638.

(8) Goldman, E. R.; Medintz, I. L.; Whitley, J. L.; Hayhurst, A.; Clapp, A. R.; Uyeda, H. T.; Deschamps, J. R.; Lassman, M. E.; Mattoussi, H. *J. Am. Chem. Soc.* **2005**, *127*, 6744−6751.

(9) Gill, R.; Willner, I.; Shweky, I.; Banin, U. *J. Phys. Chem. B* **2005**, *109* (49), 23715−23719.

(10) Medintz, I. L.; Clapp, A. R.; Brunel, F. M.; Tiefenbrunn, T.; Uyeda, H. T.; Chang, E. L.; Deschamps, J. R.; Dawson, P. E.; Mattoussi, H. *Nat. Mater.* **2006**, *5*, 581−589.

(11) Zhang, C.-Y.; Yeh, H.-C.; Kuroki, M. T.; Wang, T.-H. *Nat. Mater.* **2005**, *4*, 826−831.

(12) Patolsky, F.; Gill, R.; Weizmann, Y.; Mokari, T.; Banin, U.; Willner, I. *J. Am. Chem. Soc.* **2003**, *125* (46), 13918−13919.

(13) Medintz, I. L.; Clapp, A. R.; Melinger, J. S.; Deschamps, J. R.; Mattoussi, H. *Adv. Mater.* **2005**, *17*, 2450−2455.

(14) Snee, P. T.; Somers, R. C.; Nair, G.; Zimmer, J. P.; Bawendi, M. G.; Nocera, D. G. *J. Am. Chem. Soc.* **2006**, *128* (41), 13320−13321.

(15) Boldt, K.; Bruns, O. T.; Gaponik, N.; Eychmüller, A. *J. Phys. Chem. B* **2006**, *110* (5), 1959−1963.

(16) Mattoussi, H.; Mauro, J. M.; Goldman, E. R.; Green, T. M.; Anderson, G. P.; Sundar, V. C.; Bawendi, M. G. *Phys. Status Solidi B* **2001**, *224* (1), 277−283.

(17) Jiang, W.; Mardyani, S.; Fischer, H.; Chan, W. C. W. *Chem. Mater.* **2006**, *18* (4), 872−878.

(18) Parak, W. J.; Gerion, D.; Zanchet, D.; Woerz, A. S.; Pellegrino, T.; Micheel, C.; Williams, S. C.; Seitz, M.; Bruehl, R. E.; Bryant, Z.; Bustamante, C.; Bertozzi, C. R.; Alivisatos, A. P. *Chem. Mater.* **2002**, *14* (5), 2113−2119.

(19) Dubertret, B.; Skourides, P.; Norris, D. J.; Noireaux, V.; Brivanlou, A. H.; Libchaber, A. *Science* **2002**, *298* (29 November), 1759−1762.

(20) Wu, M. X.; Liu, H.; Liu, J.; Haley, K. N.; Treadway, J. A.; Larson, J. P.; Ge, N.; Peale, F.; Bruchez, M. P. *Nat. Biotechnol.* **2003**, *21*, 41−46.

(21) Pellegrino, T.; Manna, L.; Kudera, S.; Liedl, T.; Koktysh, D.; Rogach, A. L.; Keller, S.; Rädler, J.; Natile, G.; Parak, W. J. *Nano Lett.* **2004**, *4* (4), 703−707.

(22) Petruska, M. A.; Bartko, A. P.; Klimov, V. I. *J. Am. Chem. Soc.* **2004**, *126* (3), 714−715.

(23) Yu, W. W.; Chang, E.; Sayes, C. M.; Drezek, R.; Colvin, V. L. *Nanotechnology* **2006**, *17* (17), 4483−4487.

(24) Luccardini, C.; Tribet, C.; Vial, F.; Marchi-Artzner, V.; Dahan, M. *Langmuir* **2006**, *22* (5), 2304−2310.

(25) Ballou, B.; Lagerholm, B. C.; Ernst, L. A.; Bruchez, M. P.; Waggoner, A. S. *Bioconjugate Chem.* **2004**, *15* (1), 79−86.

(26) Sperling, R. A.; Pellegrino, T.; Li, J. K.; Chang, W. H.; Parak, W. J. *Adv. Funct. Mater.* **2006**, *16*, 943−948.

(27) Liedl, T.; Keller, S.; Simmel, F. C.; Rädler, J. O.; Parak, W. J. *Small* **2005**, *1* (10), 997−1003.

(28) Pons, T.; Uyeda, H. T.; Medintz, I. L.; Mattoussi, H. *J. Phys. Chem. B* **2006**, *110* (41), 20308−20316.

(29) Smith, A. M.; Duan, H.; Rhyner, M. N.; Ruan, G.; Nie, S. *Phys. Chem. Chem. Phys.* **2006**, *8*, 3895−3903.

(30) Sperling, R. A.; Liedl, T.; Duhr, S.; Kudera, S.; Zanella, M.; Lin, C.-A. J.; Chang, W.; Braun, D.; Parak, W. J. *J. Phys. Chem. C* **2007**, *111*, 11552−11559.

(31) Wang, K. T.; Iliopoulos, I.; Audebert, R. *Polym. Bull.* **1988**, *20*, 577−582.

(32) Lin, C.-A. J.; Sperling, R. A.; Li, J. K.; Yang, T.-Y.; Li, P.-Y.; Zanella, M.; Chang, W. H.; Parak, W. J. Submitted to *Small*.

(33) Wang, M.; Dykstra, T. E.; Lou, X.; Salvador, M. R.; Scholes, G. D.; Winnik, M. A. *Angew. Chem., Int. Ed.* **2006**, *45*, 2221−2224.

(34) Brochon, J. C., Maximum-Entropy Method Of Data-Analysis In Time-Resolved Spectroscopy. In *Numerical Computer Methods, Part B*; Academic Press: San Diego, CA, 1994; Vol. 240, pp 262−311.

(35) Lidke, D. S.; Nagy, P.; Heintzmann, R.; Arndt-Jovin, D. J.; Post, J. N.; Grecco, H. E.; Jares-Erijman, E. A.; Jovin, T. M. *Nat. Biotechnol.* **2004**, *22*, 198−203.

(36) Dahan, M.; Levi, S.; Luccardini, C.; Rostaing, P.; Riveau, B.; Triller, A. *Science* **2003**, *302* (5644), 442−445.